

Oscillatory Binary Fluid Convection in Large Aspect-Ratio Containers

O. Batiste, M. Net, and I. Mercader

Departament de Física Aplicada, Universitat Politècnica de Catalunya, Barcelona, Spain

E. Knobloch

Department of Physics, University of California, Berkeley, California 94720

(Received 27 June 2000)

Direct numerical simulations of chevrons, blinking states, and repeated transients in binary fluid mixtures with a negative separation ratio heated from below are described. The calculations are performed in two-dimensional containers for experimental parameter values and boundary conditions. Quantitative agreement with the experiments of Kolodner [Phys. Rev. E **47**, 1038 (1993)] is obtained, and the origin of the blinking and repeated transient states is elucidated.

DOI: 10.1103/PhysRevLett.86.2309

PACS numbers: 47.20.Bp, 47.20.Ky, 47.27.Te

Thermal convection in a binary fluid mixture heated from below provides an ideal system for the study of pattern formation and the transition to complex spatiotemporal dynamics [1]. In mixtures with a negative separation ratio the heavier component migrates towards the hotter boundary reducing the overall buoyancy, and convection may set in via growing oscillations. Near onset these oscillations evolve into a rich variety of time-dependent states, including extended or localized pulselike traveling wave states in annular geometry, and the so-called “chevron” and “blinking” states observed in rectangular containers of moderately large aspect ratio [2]. The “chevrons” (or counterpropagating waves) consist of a pair of equal amplitude waves propagating outwards from the cell center; when the amplitudes of these waves oscillate about the equal amplitude state the pattern is dominated alternately by left- and right-traveling waves and is then called a “blinking” state. Both states owe their existence to the presence of sidewalls, and can be understood on the basis of both bifurcation theory [3] and Ginzburg-Landau theory [4]. Of particular interest in the present paper are the “repeated transients” observed by Kolodner [5] in water-ethanol mixtures. These states consist of chevrons that grow exponentially from small amplitude without change of shape until they reach a critical amplitude at which they become unstable and collapse back to small amplitude. The experiments reveal that the dynamics of these states depend sensitively on both the aspect ratio of the system and on the Rayleigh number. At present there is no theoretical understanding of these observations.

To elucidate the origin of the repeated transients we have integrated numerically [6] the governing Boussinesq equations [1] in two-dimensional containers $\{0 \leq x \leq \Gamma, -0.5 \leq z \leq 0.5\}$ with no-slip, no-mass-flux boundary conditions [7]. The boundaries at the top and bottom are perfectly thermally conducting and the sidewalls insulating. We present the results as a function of the aspect ratio Γ of the container and of $\epsilon \equiv (R - R_c)/R_c$, where R is the Rayleigh number and R_c its critical value for the onset of the primary instability [8], for fixed values of

the remaining parameters (separation ratio $S = -0.021$, Prandtl number $\sigma = 6.97$, Lewis number $\tau = 0.0077$) specifying the experimental mixture [5]. We find that, depending on Γ , the first state that begins to grow has either odd or even parity under left-right reflection, and has the form of a chevron, as predicted by linear theory for this system [8]. The computations indicate that this bifurcation is subcritical, as expected on the basis of weakly nonlinear theory for *standing* waves in an unbounded layer [9]. In this Letter we characterize the saturated states that result and their parameter dependence.

Figure 1(a) summarizes the linear stability results, with the solid (broken) lines indicating the onset of even (odd) chevrons; Fig. 1(b) shows the corresponding linear frequencies in units of t_d^{-1} , where t_d is the thermal diffusion time in the vertical. At $\Gamma \approx 16.8$ the parity of the primary mode changes, resulting in a frequency jump. Figure 2 illustrates the sensitive dependence of the equilibrated state on the aspect ratio when $\epsilon \approx 10^{-4}$ above threshold, and the long integration times required to get reliable results. The figure shows the evolution of the mid-plane vertical velocity $v_z(x = 0.13\Gamma, z = 0, t)$ obtained by integration of the partial differential equations over $2000t_d$ after an initial transient has (almost) died out, at each of the locations indicated in Fig. 1(a). The high

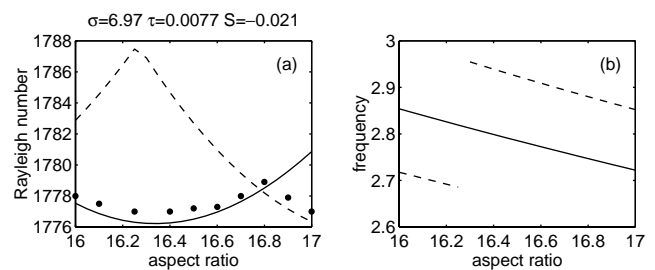


FIG. 1. (a) The critical Rayleigh number R_c and (b) the corresponding frequency ω_c for $S = -0.021$, $\sigma = 6.97$, $\tau = 0.0077$ as a function of the aspect ratio Γ . Solid (broken) lines indicate even (odd) parity chevrons. The solid dots correspond to the solutions shown in Fig. 2.

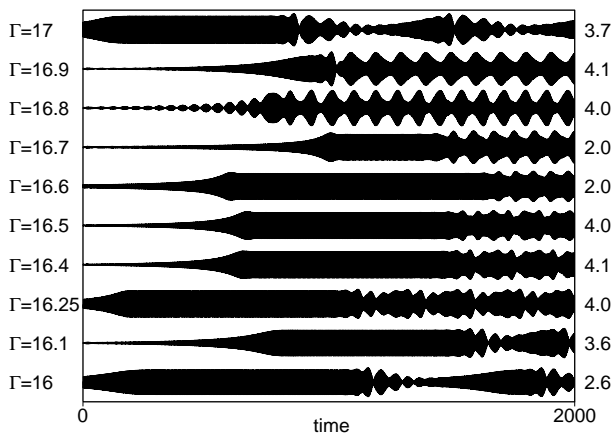


FIG. 2. An overview of the aspect ratio dependence of the equilibrated states near onset, in terms of the vertical velocity $v_z(x = 0.13\Gamma, z = 0, t)$ for comparison with Fig. 2 of [5]. The numbers at the right give $10^4\epsilon$ and correspond to the locations indicated in Fig. 1(a).

frequency uniform amplitude states correspond to nonlinear time-periodic chevron states such as the one shown in Fig. 3. The figure shows that while the temperature departure from the conduction profile remains sinusoidal at this value of ϵ this is not so for the concentration departure. As explained by Barten *et al.* [10] this is a consequence of the small value of τ . Note in particular that regions of high and low concentration departure are separated by open contours, in contrast to the temperature field. The temporary straightening of these meandering concentration contours in the cell center every half period accompanies the splitting of the central concentra-

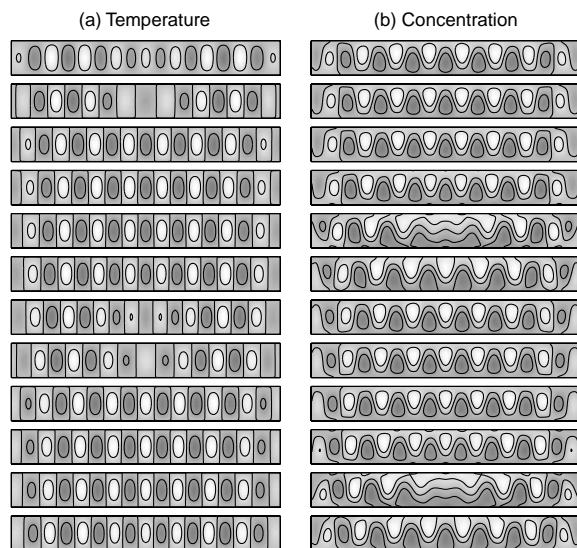


FIG. 3. Periodic even-parity chevron for $\Gamma = 16.25$, $R = 1775.5$ ($\epsilon = -4.5 \times 10^{-4}$) in terms of the contours of (a) the temperature and (b) the concentration of the denser component relative to their conduction profiles, with time increasing upwards in intervals of $0.2t_d$. For these parameter values $R_c = 1776.30$, $\omega_c = 2.819$.

tion roll into two. These properties of the concentration field are absent from the Ginzburg-Landau description of this system.

Although the chevron states are the first to appear (cf. Fig. 2) they are almost always unstable and develop into states with more complex time dependence. Symmetric periodic blinking states are invariant under evolution through half a period followed by a reflection in the center of the container, and are easily diagnosed by the 180° phase shift between the vertical velocity at two points on opposite sides of the container (Fig. 4). Figure 2 shows that these states are most easily visible near the mode crossing point $\Gamma \approx 16.8$, where the odd and even chevrons compete already at small amplitude. At other values of Γ symmetric periodic blinking states may still be present but in more restricted ranges of ϵ . Figure 5 shows an asymmetric blinking state that develops gradually from a symmetric blinking state at $R = 1776$ with increasing ϵ (Fig. 6). In this state the oscillations at the left and right differ but remain periodic with the same period, i.e., the phase difference between the two sides is constant although it now differs substantially from 180° . With further increase in ϵ this state becomes chaotic (Fig. 6), much as observed in related experiments [2] and expected theoretically [11,12]. These states are to be distinguished from the repeated transients, seen in Fig. 2 at $\Gamma = 16, 17$ and smaller ϵ , and discussed next.

For our parameter values the chevrons bifurcate subcritically at $\epsilon = 0$ and acquire stability at finite amplitude at a saddle-node bifurcation that occurs at $\epsilon_{SN} < 0$; for $\epsilon < \epsilon_{SN}$ all perturbations decay (Fig. 6). Our calculations

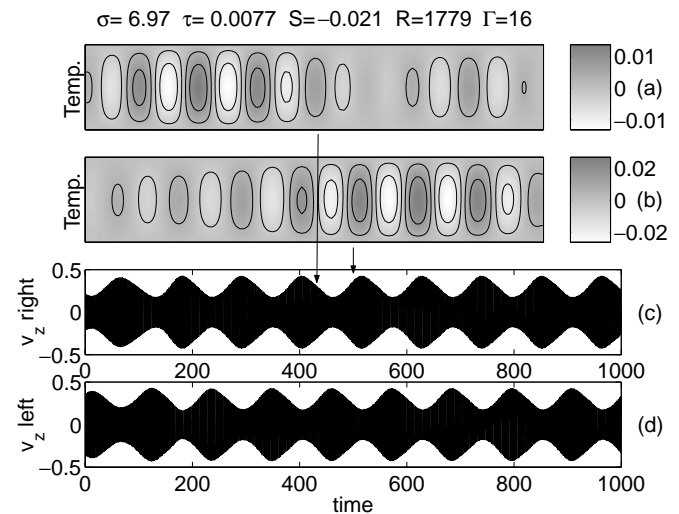


FIG. 4. Periodic blinking state for $\Gamma = 16.0$ and $R = 1779$ ($\epsilon = 8.3 \times 10^{-4}$). For these parameter values $R_c = 1777.528$, $\omega_c = 2.854$. Figures (a) and (b) show the temperature field at two instants (indicated by vertical arrows), while (c) and (d) show $v_z(x = 0.13\Gamma, z = 0, t)$ and $v_z(x = 0.87\Gamma, z = 0, t)$. The fact that (c) and (d) are identical except for a 180° phase shift is indicative of a symmetric blinking state. The blinking period is approximately 0.4 horizontal thermal diffusion times.

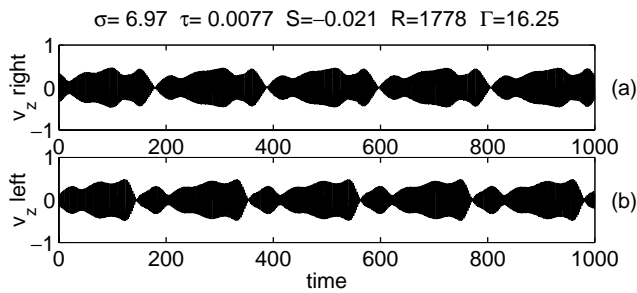


FIG. 5. An asymmetric blinking state for $\Gamma = 16.25$, $R = 1778$ ($\epsilon = 9.6 \times 10^{-4}$), showing (a) $v_z(x = 0.13\Gamma, z = 0, t)$ and (b) $v_z(x = 0.87\Gamma, z = 0, t)$. The pattern blinks during its growth phase before undergoing collapse.

reveal two distinct ways of generating symmetric blinking states, both of which are consistent with the prediction that these states are fundamentally due to a secondary Hopf bifurcation from the chevron state [13] introduced by the sidewalls [3,11]. For $\Gamma = 16.25$ this bifurcation occurs at ϵ_{Hopf} satisfying $\epsilon_{\text{SN}} < \epsilon_{\text{Hopf}} < 0$ and is supercritical (Fig. 6). Consequently, there is a narrow range of

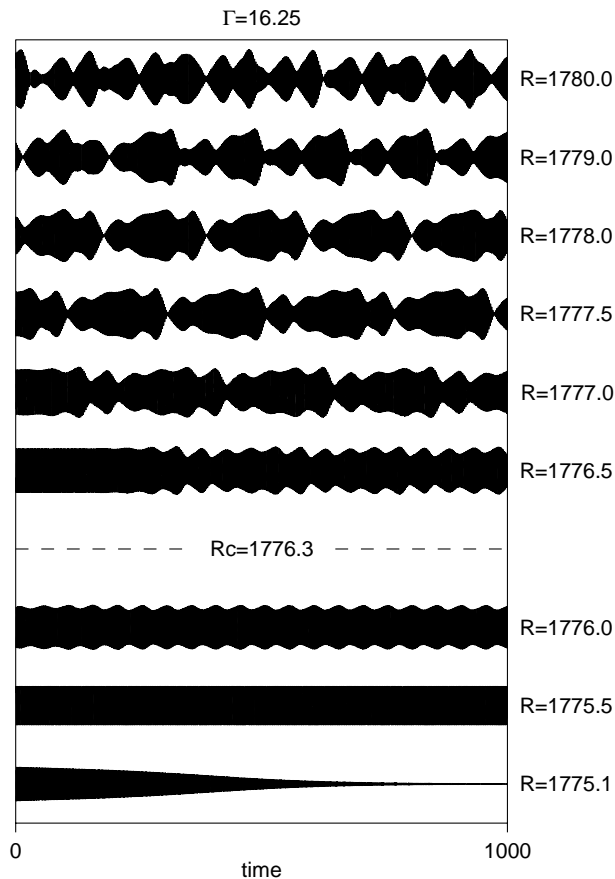


FIG. 6. Time series $v_z(x = 0.13\Gamma, z = 0, t)$ for $\Gamma = 16.25$ and different values of the Rayleigh number R . Stable chevrons are present for $R = 1775.5$ ($\epsilon = -4.5 \times 10^{-4}$), but give way to periodic blinking states when $R = 1776$ ($\epsilon = -1.7 \times 10^{-4}$) with no detectable hysteresis.

ϵ , $\epsilon_{\text{SN}} < \epsilon < \epsilon_{\text{Hopf}}$, with stable chevrons, before blinking sets in. The blinking frequency is quite small because the chevron amplitude at which the Hopf bifurcation takes place is small, while its amplitude is small because the bifurcation is supercritical. As Γ decreases the Hopf bifurcation moves past the saddle node onto the unstable part of the chevron branch below the saddle node, eliminating the stable chevrons. This is the case for $\Gamma = 16.0$ (Fig. 7). Our results for $R = 1777.2$ are suggestive of a quasiperiodic state with three independent frequencies such as might be expected from a tertiary bifurcation that stabilizes the symmetric blinking state (see below). Such tertiary bifurcations are an inevitable consequence of the passage of the Hopf bifurcation to blinking states through the saddle-node bifurcation [14]; our calculations are consistent with the conjecture that these two bifurcations coincide for Γ between 16.0 and 16.25. The period associated with the third frequency is about $1000t_d$. Such low frequencies are characteristic of this mechanism. Figure 7 suggests that the repeated transients observed by Kolodner evolve from this three-frequency state as ϵ increases. We have found such states only in the vicinity of $\Gamma = 16.0$ and $\Gamma = 17.0$, i.e., for aspect ratios differing by ≈ 1 , as expected theoretically [3] and observed in the experiments [5]. In this case symmetric blinking states are observed only after a (slightly hysteretic) transition from the three-frequency repeated transients that take place between $R = 1778.5$ and $R = 1779$ (Fig. 7). These blinking states therefore set in with finite amplitude, resulting in a longer blinking period (Fig. 4), typically $100t_d$ ($= 2.5$ h, using the estimate $t_d = 84.3$ sec [5]). This period is comparable to the

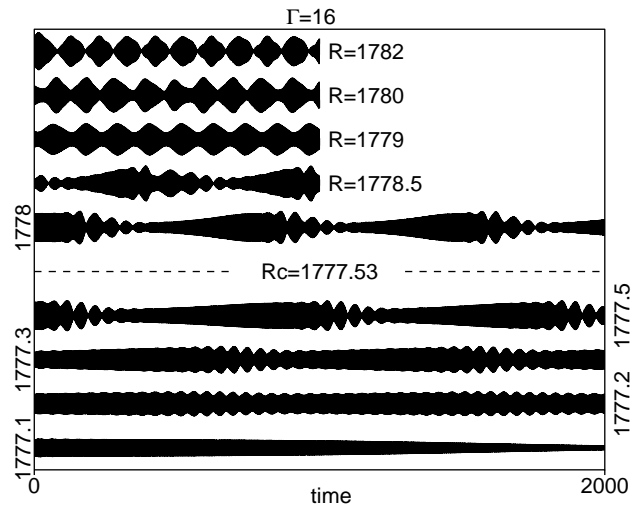


FIG. 7. Time series $v_z(x = 0.13\Gamma, z = 0, t)$ for $\Gamma = 16.0$ and different values of the Rayleigh number R . The first finite amplitude state is a three-frequency state at $R = 1777.2$ ($\epsilon = -1.8 \times 10^{-4}$). This state gives way gradually and without detectable hysteresis to repeated transient states near $\epsilon = 0$ and then to blinking states when $R = 1779$ ($\epsilon = 8.3 \times 10^{-4}$). The state at $R = 1782$ ($\epsilon = 2.5 \times 10^{-3}$) appears to have period-two modulation.

observed period. With further increase in ϵ this state appears to undergo period doubling as suggested by the time series for $R = 1782$ in Fig. 7 (cf. [11,12]).

Our calculations lead to the following interpretation of the repeated transients, described here as ϵ decreases from a symmetric blinking state at some $\epsilon > 0$. The blinking state first undergoes a Hopf bifurcation that introduces a third independent frequency into the dynamics. In the simplest case this bifurcation is supercritical, i.e., the three-frequency state bifurcates towards smaller ϵ . The new frequency is finite but decreases with ϵ as the three-frequency state approaches simultaneously the unstable large amplitude chevron state (hereafter A) and either the unstable conduction state (if $\epsilon > 0$) or the small amplitude chevrons (if $\epsilon < 0$). The character of the repeated transient is determined by the leading eigenvalues of the small amplitude state visited, hereafter B . These are $\lambda > 0$ for perturbations in the chevron fixed point subspace and the least stable eigenvalue, $-\alpha + i\beta$, $\alpha > 0$, in the perpendicular direction. A trajectory escaping from B therefore describes an exponentially growing chevron state. When this state reaches the vicinity of A it becomes unstable to symmetry-breaking oscillations which take it back near B . This is the collapse phase of the repeated transient state. The frequency of the decaying oscillations observed in the time series is given by β . Since α decreases with ϵ when $\epsilon < 0$, the collapse becomes slower and slower, as seen in Fig. 7, but is still finite when the three-frequency states disappear in a global bifurcation at $\epsilon^* < 0$ and the system makes a hysteretic transition to the conduction state. The fact that α decreases with ϵ makes it likely that the Shil'nikov condition $\lambda/\alpha > 1$ holds at ϵ^* , resulting in chaotic repeated transients prior to their disappearance [12]. This possibility apparently does not occur in Fig. 7 but may occur in the experiments. Note that since $\lambda \propto |\epsilon|$ only periodic repeated transients will occur if the global bifurcation occurs too close to $\epsilon = 0$.

Symmetric blinking states are easiest to find near mode crossing points ($\Gamma \approx 16.8$). However, the location of these points depends quite sensitively on the system parameters and in particular on the additional dissipation due to the neglected no-slip walls in the third direction. Consequently, differences between the experimental results and our calculations may be primarily due to differences in the location of these points. Indeed, Kolodner finds that blinking states persist down to small amplitudes for $\Gamma = 16.63$ and $\Gamma = 17.63$ when the width $\Gamma_y = 3.0$, and for $\Gamma = 16.25$ and $\Gamma = 17.25$ when $\Gamma_y = 4.9$. A detailed description of our results and their theoretical interpretation will be given elsewhere [15].

This work was supported by the U.S.-Spain Science and Technology Joint Research Program (Fulbright Grant No. 99231) and DGICYT under Grant No. PB97-0683.

Additional support from a National Science Foundation Grant No. DMS-9703684 is acknowledged. Computer time was provided by CEPBA.

-
- [1] M. C. Cross and P. C. Hohenberg, *Rev. Mod. Phys.* **65**, 851 (1993).
 - [2] P. Kolodner, C.M. Surko, and H. Williams, *Physica (Amsterdam)* **37D**, 319 (1989); V. Steinberg, J. Fineberg, E. Moses, and I. Rehberg, *ibid.* **37D**, 359 (1989).
 - [3] G. Dangelmayr and E. Knobloch, in *The Physics of Structure Formation*, edited by W. Güttinger and G. Dangelmayr (Springer-Verlag, New York, 1987), pp. 387–393; *Nonlinearity* **4**, 399 (1991); G. Dangelmayr, E. Knobloch, and M. Wegelin, *Europhys. Lett.* **16**, 723 (1991).
 - [4] M. C. Cross, *Phys. Rev. A* **38**, 3593 (1988); *Physica (Amsterdam)* **37D**, 315 (1989).
 - [5] P. Kolodner, *Phys. Rev. E* **47**, 1038 (1993); see also P. Kolodner and C.M. Surko, *Phys. Rev. Lett.* **61**, 842 (1988).
 - [6] G. E. Karniadakis, M. Israeli, and S. A. Orszag, *J. Comput. Phys.* **97**, 414 (1991).
 - [7] H. Yahata, *Prog. Theor. Phys.* **85**, 933 (1991); L. Ning, Y. Harada, and H. Yahata, *ibid.* **97**, 831 (1997); D. Jacqmin and D. Heminger (unpublished).
 - [8] O. Batiste, I. Mercader, M. Net, and E. Knobloch, *Phys. Rev. E* **59**, 6730 (1999).
 - [9] W. Schöpf and W. Zimmermann, *Europhys. Lett.* **8**, 41 (1989); T. Clune and E. Knobloch, *Physica (Amsterdam)* **61D**, 106 (1992).
 - [10] W. Barten, M. Lücke, W. Hort, and M. Kamps, *Phys. Rev. Lett.* **63**, 376 (1989); W. Barten, M. Lücke, M. Kamps, and R. Schmitz, *Phys. Rev. E* **51**, 5636 (1995).
 - [11] P. C. Hirschberg and E. Knobloch, *Physica (Amsterdam)* **90D**, 56 (1996).
 - [12] E. Knobloch, in *Pattern Formation: Symmetry Methods and Applications*, edited by J. Chadam, M. Golubitsky, W. F. Langford, and B. Wetton, Fields Institute Communications (AMS, Providence, RI, 1996), Vol. 5, pp. 271–279. Any chaos due to breakdown of the three-frequency motion would be much milder.
 - [13] Strictly speaking this bifurcation is a Neimark-Sacker bifurcation. However, in the following we do not distinguish between Hopf bifurcations of equilibria and of periodic orbits, since resonance phenomena appear to play little role in the observed dynamics.
 - [14] W. Langford, in *Nonlinear Dynamics and Turbulence*, edited by G. Barenblatt, G. Iooss, and D. Joseph (Pitman, Boston, 1983), pp. 215–237; see also J. Guckenheimer and P. Holmes, *Nonlinear Oscillations, Dynamical Systems and Bifurcations of Vector Fields* (Springer-Verlag, New York, 1984).
 - [15] O. Batiste, E. Knobloch, I. Mercader, and M. Net (unpublished).